ESA's USE OF THE 1 M ZEISS TELESCOPE FOR SPACE DEBRIS OBSERVATIONS

A. Massart, G. Janin and W. Flury

European Space Operations Centre, Darmstadt, Germany

ABSTRACT

The 1m Zeiss telescope installed at the Teide observatory in Tenerife was upgraded for the observation of space debris. The performance of the telescope and its CCD camera is briefly reviewed together with the data processing system. After assessing the characteristics of debris at geostationary altitudes, the paper reviews the algorithms that will be used for the detection of objects on CCD frames and the determination of their orbit. A concept for a survey of the geostationary orbit is then presented.

1. THE TELESCOPE

The telescope is installed in the Optical Ground Station (OGS) of ESA at the Teide observatory of the Instituto Astrofisica de Canarias, at Izaña (Tenerife, Spain). The site (longitude: 343.5° E, latitude: 28.5° N, altitude: 2393m) provides seeing conditions of sub-arcsec quality, and yearly statistics indicate that there are in average 70% of clear nights.

The OGS was established by ESA in the frame of the Data Relay and Technology Mission for the in orbit check-out of the payload of the ARTEMIS spacecraft. It consists of an observatory building with a rotating dome, the telescope with different optical systems, special optical test equipment for the Artemis payload test, and a control centre.

The telescope is a Zeiss 1m Ritchey - Chretien/Coudé telescope supported by an English mount. It can be operated with three optical configurations: the basic Ritchey-Chretien system, the modified Ritchey-Chretien system with focal reducer, and the Coudé system. The basic Ritchey-Chretien system and the Coudé system can be used for astronomical observations. The Coudé configuration will be used for the in orbit check out of the optical payload of ESA's Artemis spacecraft. The modified Ritchey-Chretien system (spherical secondary mirror and focal reducer) will be used for space debris observations. In the space debris configuration, the focal length of 4.47m provides an unvignetted flat field of view of 1.2°. The optical transmissivity is better than 70% in the 450nm to 950 nm spectral range and the diameter of the 80% light concentration of a point source is 0.7".

The telescope control system, originally developed for astronomical observation, has been upgraded to meet the operational requirements associated with the observation of space debris and with the in orbit tests of the Artemis payload. In a special operation's mode, the Telescope Control Computer (TCC) is slaved to a Central Control Computer (CCC) via an RS232 link. In this mode, the CCC provides the TCC with pointing directions which correspond to a satellite trajectory or to the expected track of a space debris. The TCC executes the commands and feeds back to the CCC the actual pointing parameters of the telescope. The link is also used to control the telescope focus and, more generally, to monitor the telescope and dome status parameters. This external control loop (TCC-CCC) works at 10 Hz, whereas the internal control loop of the TCC and of the associated drives controllers works at 50 Hz. This ensures at all times a smooth movement of the telescope. The telescope drives permit slew rates of up to 2°/sec and accelerations of 0.5°/sec^2. The TCC pointing (or mount) model permits to position the telescope to better than 10". The tracking error is less than 2"/h. The rotation of the dome and the position of the sight shutters is automatically controlled by the TCC and follows the line of sight of the telescope. A GPS receiver provides the UTC time.

The telescope is equipped with a prontor E100 Iris shutter which is used for exposures longer than 125 msec. Later, a rotating disk shutter will be installed that permits exposures as low as 5 msec.

2. THE CCD CAMERA

For the observation of space debris the telescope is equipped with a CCD camera of 4k x 4 k pixels. The detector consists of a mosaic of four EEV 42-40 devices. Each device has 2048x2048 pixels of 13.5 x 13.5 μm^2. The detector, located in the focal plane of the telescope, covers a field of view of 1° with an image scale of 0.6"/pixel. The flatness of each device is better than 10 μm (peak to valley) and that of the mosaic is better than 20 μm.

The detector is mounted in the evacuated chamber of a Dewar together with the preamplifiers. The cryostat coolant (liquid nitrogen) together with the thermal control (heaters) holds the temperature of the chips constant at 160°K (± 1°K) so that the dark current generated by the CCD during an exposure is negligible (< 2 e$^-$/ hour per pixel).

The devices are front illuminated and cover the spectral range 400 nm to 1050 nm with a quantum efficiency better than 40% at 700 nm. The photo response non uniformity is less than 2 %. Defective pixels (hot or cold) are limited to 100 per chip. The full well capacity is 150,000 electrons per pixel. The charge transfer efficiency is better than 0.99999.

To keep the CCD read out time short, each EEV device is equipped with two output amplifiers (responsivity: 4 $\mu V/e^-$) and is operated by an AstroCam 4400 controller. The read out of the four devices is synchronised to 100 ns and the data output by the 4 x 2 channels are multiplexed on an S bus link and transferred to a Sun workstation where the image is reconstructed in memory and displayed.

To ensure adequate dynamic range, the controller digitises the voltage data to 16 bits, using a correlated double sampling circuit (dual slope integrator method). The pixel read out rate can be set between 6 µs and 50 µs. Each controller channel is optimised for a different read out rate. The read out noise of 4 e^- at 25 µs/pixel reaches 8 e^- at the fastest rate of 6 µs/p. The overall system gain is such that, at the fastest read out rate, the least significant bit corresponds to 1 e^- (high gain) and 8 e^- (low gain), whereas at the 25 µs/p rate it corresponds respectively to 0.25 e^- and 2 e^-. The 4k x 4 k image frame is transferred to the workstation's memory in 13 sec.

The operator interfaces with the camera from the Sun workstation. The user interface is programmed in IDL and uses AstroCam's proprietary "C" interface to dialogue with the camera. This user interface permits to acquire exposures, visualise the images, evaluate their quality, and store them on disk in FITS format. It also provides basic analysis and image manipulation functions.

In between exposures, the camera is automatically set in permanent flushing mode.

To reduce the amount of data to be transferred to the work station, the data can be binned in pixel and line directions. The CCD can also operate in windowed mode (up to 2 windows can be specified in one or more chips), in which case the windows are read out one after another and stored as two sub files in a common data file.

The UTC time synchronisation is ensured by the IRIG B signal obtained from the GPS receiver. Time events are logged and stored together with the image data. To satisfy the stringent orbit determination requirement on the epoch of the exposures when using the iris shutter, the image is "smeared" during the opening and closing of the shutter by flushing lines at a high rate. This ensures that all pixels are exposed for the same duration and that any signal received during the opening or closing of the shutter disappears in the background by spreading it over a large number of pixels. This mechanism provides an exposure time accuracy better than 1 msec.

3. THE DATA PROCESSING SYSTEM

Fig. 1 illustrates the control and data processing system. The operation of the CCD camera (control, exposure taking and transfer to the work station) is directly controlled from the CCC. These activities are to be synchronised with the operations of the telescope (controlled by the TCC). Hence the TCC-CCC link permits to integrate in the CCC all facilities required to operate the telescope and the camera in a coherent and user friendly system. This integrated system, or level-1 control, delegates to the level-2 control facilities (TCC and CCD camera subsystems) the execution of the relevant tasks. It also minimises the interventions of the operator on the individual components so that he can concentrate on his observations. The level-2 control takes also care of the safety aspects of the subsystems: in case of problems, it takes immediately the measures necessary to safeguard the system and then reports alarms or out of limits to the level-1 control to inform the operator.

The following observation modes, associated with the detection of space debris, are supported: sky surveys for the detection and identification of new objects, tracking of newly discovered objects in order to establish their orbit, and observations of "known" objects in order to periodically refine their trajectory. The tasks associated with these modes of observations are distributed over two workstations: the on line processing facilities implemented in the CCC and the off line software implemented in the Observation Processing Computer (OPC).

The "on line" processing facilities associated with the exposures can be classified in four groups. The first set contains the tools required to visualise the images, to extract the regions of interest and to verify the optimal performance of the observation system. The second group covers the facilities associated with the detection of objects and the determination of their CCD coordinates. In the third group are the facilities associated with the computation of the inertial coordinates, the identification of objects, and the determination of an initial orbit so that newly detected objects can be re-acquired later during the night or the following night. The fourth group contains the tools the tools that expand the daily observation sequences (generated off line in the OPC) into the appropriate sequences of commands for the telescope and the CCD camera, and the monitoring facilities associated with the follow up of their execution.

Other general facilities are also implemented in the CCC: for example, the facilities required to communicate with the TCC, the CCD camera and the OPC.

The " off line" processing facilities can also be classified in four groups. The first group contains those facilities associated with calibrations activities: they cover the production of generic bias and flat fields for the CCD frames pre-processing, and the determination of the parameters mapping the CCD coordinates into celestial coordinates. The second set is concerned with the final data reduction of the exposures, the orbit determination, and the final identification of the objects. The third set is dedicated to the preparations activities (long, medium and short term planing tools). Finally, the fourth group contains those tools associated with the various catalogues that are part of the system (geostationary objects input catalogue, newly

discovered geostationary objects catalogue, planetary ephemerides, star catalogues,...).

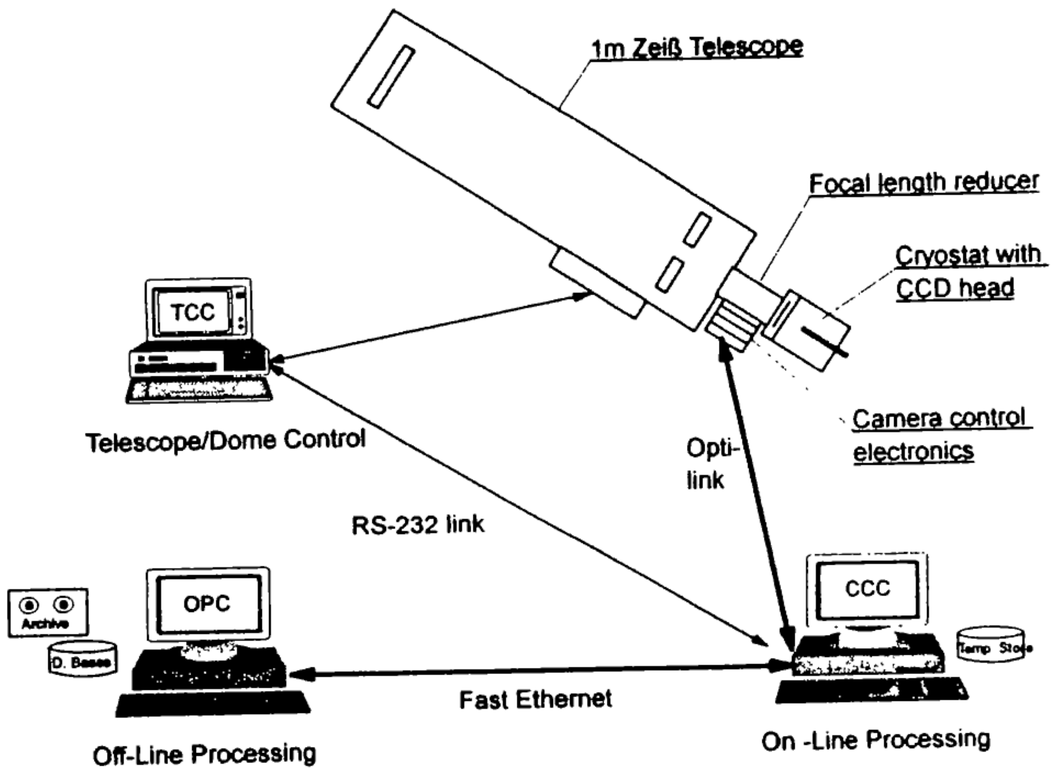

Fig. 1 Space debris observation system

4. OBJECTS IN GEOSTATIONARY ORBIT

A query of ESOC's DISCOS data base produced ca. 670 objects in or near the geostationary ring. This catalogue, based on the NASA Two-Line Elements, has been complemented by the RAE Table of Earth Satellites. Only about a third of these 670 catalogued objects are operational spacecraft; the rest are rocket upper stages, apogee boost motors or abandoned spacecraft. The present geostationary objects data base (GEO) does not contain fragments from break-ups, although at least two such break-ups have occurred: a Titan upper stage (February 1992) and an Ekran satellite (June 1978). Furthermore, a survey made by NASA, totalising more than 250 hours of observation between 1992 and 1994, with a 32cm Schmidt telescope (limiting magnitude $m_v = 17$) on Maui/Hawaii, indicates that a measurable debris population exists in or near the geostationary orbit: nearly 30 % of the objects detected were not catalogued.

The steady increase in the number of catalogued objects in the geostationary and the super-geostationary ring is shown in figure 2. The key orbital parameters of these objects are shown in figures 3 and 4. It is seen that all objects have low ($\leq 15°$) inclination, and that the right ascension of their ascending node lie mainly in the interval (330°, 90°): this is due to the luni-solar perturbations which cause a periodic change of the inclination of uncontrolled objects from 0° to 15° and back in 54 years . This is also apparent in fig.5 which shows the projection of the orbit pole of all objects in the GEO data base. In this plot, the distance from the centre (radius) represents the inclination of the orbit (4 concentric circles for I = 5°, 10°, 15° and 20°) and the angle (0° to 360°) is the R.A. of the ascending node - 90°. In fig. 5 the operational spacecraft are initially clustered around the centre but drift away on a 54 year circle when they run out of fuel. On figures 3 to 5, one notices high concentration of objects in particular regions.

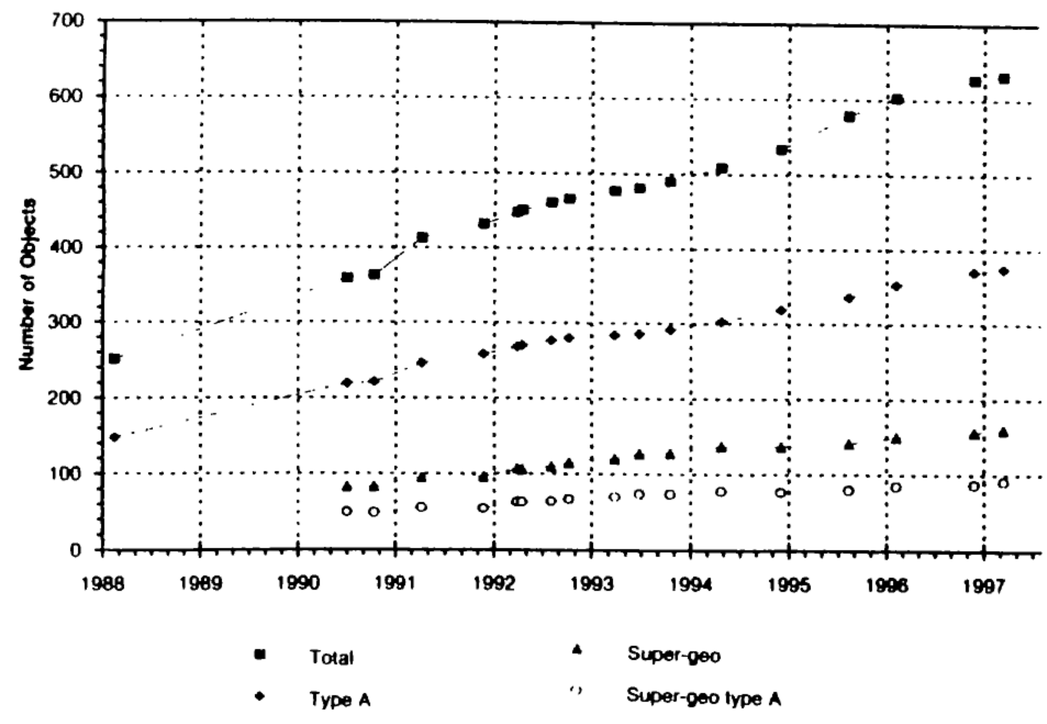

Fig. 2 Objects in geostationary and super geo orbit

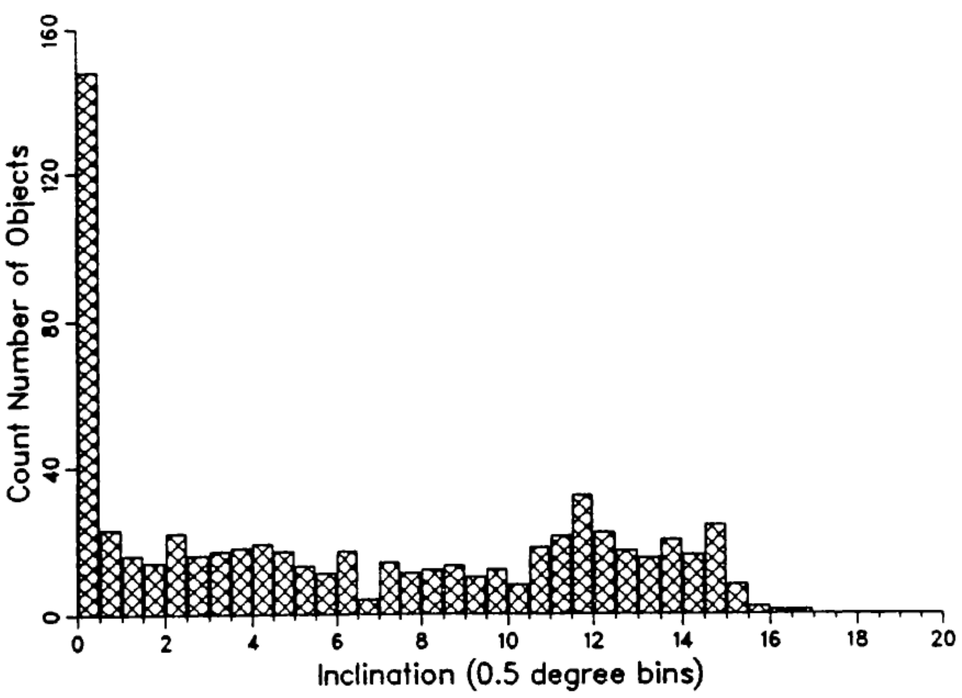

Fig. 3 Inclination distribution

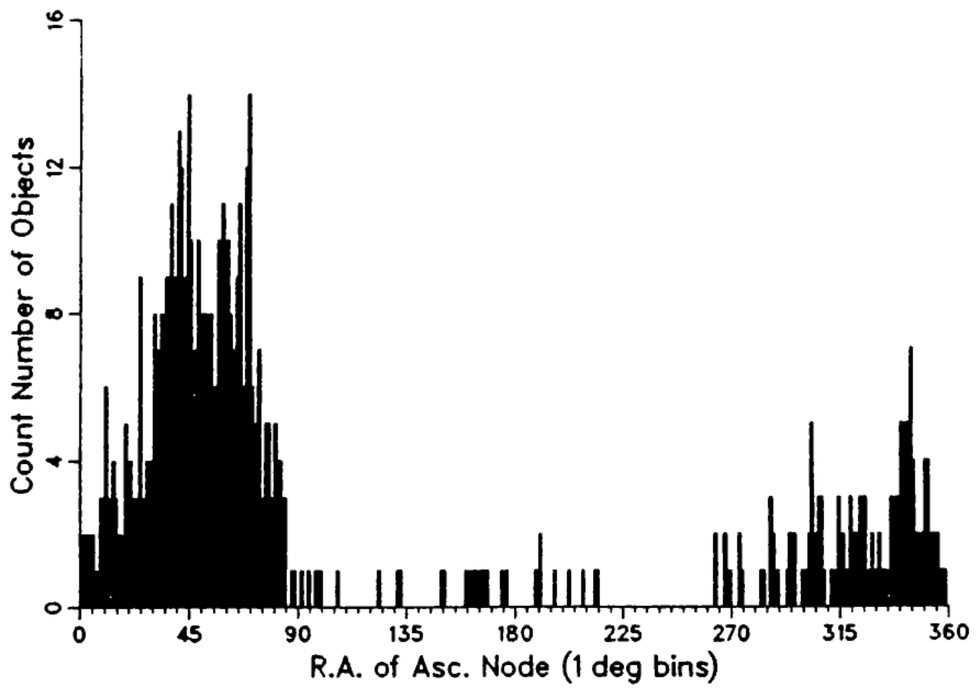

Fig. 4 R.A. of ascending node

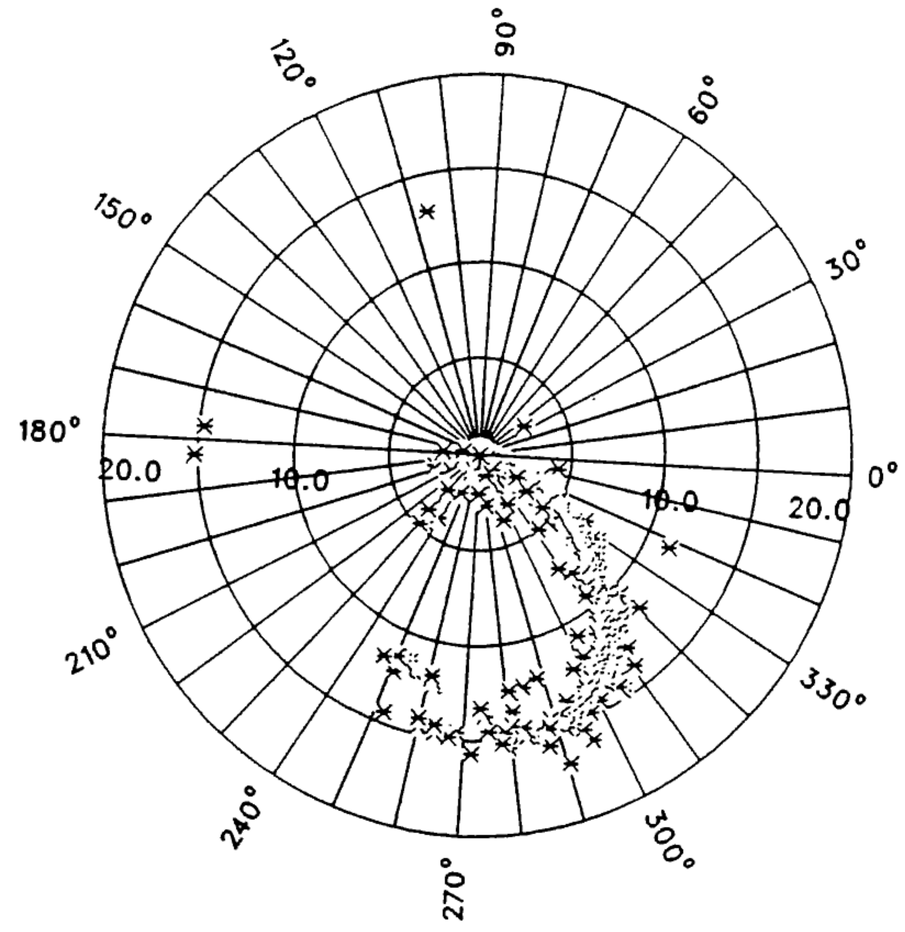

Fig. 5 Orbit pole of geostationary objects

The E/W drift rate of the objects with respect to a rotating earth is illustrated in table 1. As expected, most catalogued objects have small drifts and even those with larger drifts can usually be observed for a few nights.

< 0.1° / d	< 1° / d	< 10° / d	< 30° / d
272	378	565	625

Table 1. Number of objects as function of daily drift rate

With respect to the CCD detectors, the drift rate may reach 5"/sec when the telescope is parked (drives off) and 17"/sec when the telescope is in the sidereal tracking mode.

The brightness of the catalogued objects vary greatly, with $10 < m_v < 20$. Large structures may reach the 10 th magnitude whereas smaller compact spacecraft will be closer to the 17 th magnitude, depending on their illumination conditions.

5. OBJECT DETECTION

The limiting factors for optical observations are the apparent magnitude and the angular velocity of the objects of interest.

The object signal strength as seen by the detector will depend on the tracking scheme used during the observation and of the telescope/CCD characteristics. To achieve the best possible S/N ratio, the exposure duration should be of the order of the pixel crossing time; during the rest of the time the pixel will accumulate noise from the sky background and from the detector.

The large amount of data to be processed (32 Mbytes per frame, and 2 frames per minutes in average) requires an efficient object detection algorithm. The main task of the detection consists of the discrimination between the 'objects of interest' and the remaining objects on the frame (i.e. the 'stellar' background).

A study carried out for ESOC by the AIUB recommends to use the "masking" technique, instead of the more classical substraction technique which increases the noise and is very time consuming as it requires a precise transformation between the frames to make background stars coincide in both frames. The masking technique is comparing 'search' frames with a 'reference' frame of the same region of the sky by masking the sky background (generated from the 'reference' frame) onto the search frames. The digital mask constructed from the reference frame is slightly larger than the background object so that a resampling of the pixels is not necessary. Then, depending on the selected observation strategy, the same mask can be applied for a number of exposures.

Once the background objects have been masked, the resulting frames are searched for 'real' objects. For this, the local mean background (mainly sky) and its standard deviation σ are determined and a tresholding mechanism is applied to discriminate 'object' pixels from 'background' pixels:

$$\text{threshold} = \text{mean background} + c.\ \sigma \qquad (1)$$

The pixels belonging to the same object are then collected and the characteristics of the object are computed: position, intensity and shape.

The selection of 'c' in (1) is critical to the procedure. If 'c' is too low there will be false detections, i.e. background noise will be recognised as objects. On the other hand, if 'c' is unnecessarily large the tresholding will miss 'faint' objects.

The use of a filter in the tresholding mechanism permits to decrease significantly the value of 'c' while still avoiding false detections. Table 2 results from many simulations and gives the lowest allowed threshold (i.e. value of 'c') as function of the filter size. Although the table shows the clear advantage of the 3x3 filter, one should note that the optimum filter size depends on the actual size (in pixels) of the object and that this size results from many factors such as tracking scheme, exposure duration, binning factor,... Hence, the final selection of the optimum parameters for the algorithms will result from the commissioning of the space debris observation system.

Filter size	Lowest allowed threshold ©	limiting magnitude of detectable objects (m_v)
3 x 3	1.3	19.2
2 x 2	1.8	19.0
None	2.7	18.7

Table 2. Minimum threshold and limiting magnitude as function of filter size.

6. ORBIT DETERMINATION

Having detected "uncatalogued" objects on search frames, it is necessary to determine their orbit so that the new objects can be tracked and recovered at a later time.

In the AIUB study, the performance of various orbit determination algorithms was evaluated. These algorithms use a set of observations (t_i, α_i, δ_i, I = 1, n) of an object in order to determine or improve the orbital elements. The study covered the use of one, two, three or more observations, spanning short or long orbital arcs, and this with different measurement accuracies. With one observation of a known object, the along track error can be corrected by shifting the mean anomaly of an otherwise fixed set of orbital elements. When two observations of an uncatalogued object are available, orbit determination is carried out under the assumption that the orbit is circular. With three observations, the six keplerian elements are determined. Finally, statistical methods are used to compute an accurate set of orbital elements when three or more observations, spanning long orbital arcs, are available.

The circular orbit determination method is well suited for the identification and tracking of newly discovered (i.e. uncatalogued) objects. Figure 6 indicates, for different telescope field of view sizes, after how long an object (in an eccentric orbit) can still be recovered, using the results of a circular orbit determination from 2 observations separated by 1 min (solid line) or 10 min (dotted line). Even for large eccentricities (0.1), which is atypical of geostationary or super geostationary objects, a circular orbit determination still permits to acquire the object one hour later in a telescope with a 1° field of view.

7. OBSERVATION SCENARIO

The algorithms described above for object detection, identification and orbit determination, together with the key characteristics of the telescope and of the CCD camera, lead to the following observation scenario.

A few exposures separated by ca. 30 sec are taken and preprocessed. One of these exposure is selected as 'reference' frame and used to generate a mask. The mask is applied to the 'search' frames and these masked exposures are then searched for objects. For each detected object, the CCD position is compared with that predicted for the catalogued objects and the new (i.e. uncatalogued) objects are identified on the exposures. The objects appearing in at least two search frames are kept and their inertial position is computed. These positions are then used to compute a circular orbit and generate ephemerides. After 15 to 30 min, two further samples of the new objects are taken and t he residuals (predicted - observed) are used to validate the circular orbit. Should the residuals be too large, the elliptic orbit determination option can be used to obtain more accurate predictions. The computed orbits are continuously improved by taking hourly exposures of the new objects for the rest of the night. The following night, the objects will be observed again and a "final" statistical orbit determination can be made by combining observations of different nights.

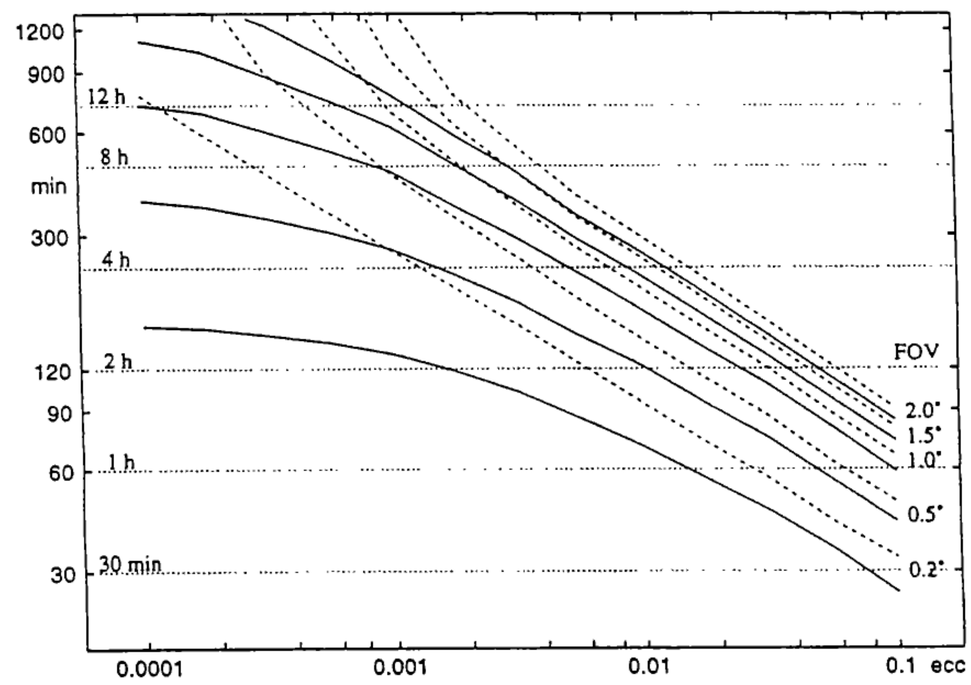

Fig. 6 Time after which an object can be reacquired within a given telescope FOV, using predictions from a circular orbit determination

The above scenario for object identification and orbit determination depends on the mode of operation of the telescope and of the CCD camera. The telescope can be operated either in sidereal tracking mode, giving CCD exposures with a fixed star background, or in parked mode (drives off), where the constant pointing direction in the earth fixed frame gives images where the stars are trailed.

In sidereal tracking, the reference frame required to eliminate the background objects from the search frames can be reused for many exposures and this reduces significantly the computer load . Unfortunately, on the exposures, the objects are trailed and the S/N ratio is reduced.

In parked mode, the S/N ratio is generally higher since a 'geostationary' objects illuminates the same pixel for a longer time interval. The draw-backs are that the mask must regularly be extended to compensate for the earth rotation and that the background stars are trailed.

When searching for objects, the CCD data will normally be

binned in order to speed up the read out, and possibly improve the S/N ratio. Once new objects have been detected, their accurate positions are obtained by taking full resolution exposures but transferring and processing only smaller windows around the expected positions of the objects.

8. SURVEY OF THE GEOSTATIONARY ORBIT

In its 12th meeting, the IADC recommended the coordination of an international observation campaign of the geostationary orbit. The survey is scheduled to start in autumn 1997 with the participation of different countries. ESA/ESOC will contribute to this campaign with the 1m Zeiss telescope in Tenerife.

The main objective of the survey is to determine the extent and the character of debris in or near the geostationary orbit. In a first phase, the survey will be limited to the characterisation of uncatalogued objects as to brightness and key orbital parameters (inclination, right ascension of ascending node, mean motion). Later, it will be attempted to characterise the GEO debris population according to generic type of motions (libration, circulation,...) and to assess the completeness and the accuracy of the catalogue of geostationary objects.

For a minimum elevation of 20° above the horizon, the geostationary sector visible from Tenerife covers the longitude interval (- 74°, + 42°). To cope with the 15° inclination motion of the geostationary objects, a band of ± 15° around the equator will be scanned. To cover this area with the (0.7° x 0.7 °) field of view of the Zeiss telescope requires 7000 CCD frames (or telescope pointing directions). Since the telescope can take ca. 600 exposures per night, the survey of the visible part of the geostationary ring could theoretically be completed in three periods of two weeks (a minimum of three exposures are required for each sky location: one reference frame and two search frames). However, this does not yet account for the tracking of newly discovered objects and the determination of their orbit. Hence, it is planned to use 110-120 observation nights, split in monthly campaigns of two weeks around the new moon: this assumes that, in average, 5 min is spend at each location.

To commission the space debris observation system, the area with a high density of catalogued objects will be surveyed first. For example, in the ± 0.5° band around the equator, one expects to find one catalogued object every 6th pointing direction, compared to 1 in 35 elsewhere in the geostationary ring.

With the 1m Zeiss telescope the survey will take the form of a succession of observation campaigns of one month duration. Each campaign will have three phases: a planning phase, the observation campaign itself, and the analysis phase. The two first campaigns will have an experimental character. They will be used to validate the 'integrated' space debris observation system, to tune the detection algorithms by optimising processing parameters and to identify the most appropriate mode of operation of the telescope and the CCD camera.

When sufficient experience will have been gained with the 1m Zeiss telescope during the geostationary survey, it is planned to analyse the debris situation in the Ariane geostationary transfer orbit.

9. REFERENCES

1. Flury, W., *Collision Probability and Spacecraft Disposition in the Geostationary Orbit*, Adv. Space Res, Vol.11, No 12, pp(12) 67- (12)79, 1991.

2. Janin, G., *Log of objects near the geostationary ring*, Issue 17, March 1997.

3. Schildknecht,T., Hugentobler, U., Verdun, A., and Beutler, G., *CCD Algorithms for Space Debris Detection*, Final Report of the AIUB for ESA/ESOC contract no 10623/93/D/IM, September 1995.

4. Carl Zeiss Jena, *1m RCC Telescope*, Product Information Note, agv-khr, July 1993.

5. Carl Zeiss Jena, *1m Telescope Control System*, Product Information Note, agv-khr, July 1993.

6. Carl Zeiss Jena, *12.5m Observatory Dome*, Product Information Note, agv-khr, July 1993.

7. Carl Zeiss Jena, Sira electro-optics and EEV Solid State Imaging, *Design Data Package for the Space Debris Camera*, Issue 4, produced for ESA/ESOC contract no 10709/94/D/IM, February 1997.